Excitation-emission fluorescence-kinetic data obtained by Fenton degradation. Determination of heavy-polycyclic aromatic hydrocarbons by four-way parallel factor analysis

Maira D. Carabajal, Juan A. Arancibia,* Graciela M. Escandar*

Instituto de Química Rosario (CONICET-UNR), Facultad de Ciencias Bioquímicas y Farmacéuticas, Universidad Nacional de Rosario, Suipacha 531 (2000) Rosario, Argentina.

* Corresponding authors.

E-mail addresses: escandar@iquir-conicet.gov.ar (G.M. Escandar), arancibia@iquir-conicet.gov.ar (J.A. Arancibia).

ABSTRACT

For the first time, a simple and environmentally friendly third-order/four-way calibration was applied for the simultaneous determination of five heavy-polycyclic aromatic hydrocarbons (PAHs) in interfering environments. The kinetic evolution of the Fenton degradation of benzo[*a*]pyrene, dibenz[*a*,*h*]anthracene, benzo[*b*]fluoranthene, benzo[*k*]fluoranthene and benz[*a*]anthracene was followed by recording full excitation-emission fluorescence matrices (EEFMs) of the samples at different reaction times, obtaining third-order EEFM-kinetic (EEFM-K) data. The sensitivity of the method was increased by carrying out the reaction in the presence of methyl-β-cyclodextrin. The four-way parallel factor (PARAFAC) algorithm, which was used for data processing, exploits the second-order advantage, allowing analyte concentrations to be estimated even in the presence of an uncalibrated fluorescent background. The clear superiority of the applied approach in comparison with second-order/three-way calibration performed with unreacting EEFMs is demonstrated, using two sets of samples with foreign compounds with particular spectral profiles. In one of the latter sets, the existence of a third-order advantage was explored and discussed. The feasibility to directly determine parts-per-trillion concentration levels of PAHs after a very simple solid-phase extraction with C18 membranes is established with natural water samples containing uncalibrated constituents.

Keywords: Excitation-emission fluorescence matrix-kinetic data; Third-order/four-way calibration; Third-order advantage; Fenton reaction; Heavy-polycyclic aromatic hydrocarbons

1. Introduction

Heavy-polycyclic aromatic hydrocarbons (PAHs), which are characterized by bearing more than four benzene rings in their structures, are environmental pollutants of concern because they represent a serious carcinogenic risk to humans [1,2]. A distinction is also made in the literature between low- and high-molecular weight PAHs. The latter, with a molecular mass larger than 300 Da, are of great environmental and toxicological importance [3]. The adverse effects of many PAHs justify the many efforts of regulatory agencies to monitor and control their presence in the environment [4].

PAHs exhibit significant fluorescence in solution and numerous methods based in this type of signal have been developed for their determination in different matrices. In addition, the successful coupling of the sensitivity of molecular fluorescence with the selectivity of multivariate calibration has given rise to a variety of methods for the simultaneous determination of PAHs at trace levels in very interfering environments [5–8]. The reported methods were based on second-order data obtained, for example, through measurements of excitation-emission fluorescence matrices (EEFMs) and elution time-fluorescence emission wavelength matrices. These works, as most literature ones on multiway calibration, concentrate in second-order/three-way data [9,10]. Potentially more helpful data are three-dimensional arrays measured for each sample, which can be arranged into a four-way object [9]. Calibration of analytes based on these data can be called third-order/four-way calibration. In order to clarify the nomenclature, Table S1 of Supplementary Material provides a classification of the hierarchy of data and calibrations.

As second-order/three-way calibration, four-way data arrays exhibit the so-called "second-order advantage", offering additional sensitivity and selectivity [11]. Recall that the second-order advantage refers to the possibility of quantitating an analyte even in the presence

of potential interferences not modelled in the calibration stage, and represents an immensely useful and powerful property of multiway calibration [12].

However, although modern analytical instrumentation may produce third-order data in an easy way, the usefulness of third-order/four-way calibration has been relatively unexplored. Approaches to obtain third-order/four-way data involve the recording of full excitation-emission fluorescence (or phosphorescence) matrices of a sample as a function of reaction time [13–18], pH [19], volume of quencher [20], or decay time [21]. Multidimensional data formats combining spectral and kinetic information display a remarkable potential for chemometric analysis.

In the present paper, taking advantage of the fluorescent properties of PAHs and of their easy degradation by a Fenton reaction, a new third-order/four-way method for the determination of benzo[*a*]pyrene (BaP), dibenzo[*a*,*h*]anthracene (DBA), benzo[*b*]fluoranthene (BbF), benzo[*k*]fluoranthene (BkF) and benz[*a*]anthracene (BaA) was developed. The Fenton reaction (oxidation with hydroxyl radicals generated by hydrogen peroxide and ferrous ions) was selected because it is one of the most employed chemical techniques for the initial oxidation stage of PAHs degradation during wastewater, soil and sludge treatments [22,23]. EEFMs were measured in a matter of seconds with a fast-scanning spectrofluorimeter and were successfully processed with four-way PARAFAC [14].

In order to obtain an appropriate kinetic behaviour and high initial fluorescence of the analytes, the experimental variables were optimized. The results obtained with the proposed strategy were discussed and compared with those provided by unreacting EEFMs processed with second-order/three-way calibration. This comparison was carried out on samples with and without potential interfering agents. In all cases, it was shown that third-order/four-way calibration improves the figures merit of the method. In a particular case where the selected interferents display emission spectra which are very similar to that of one of the analytes, its

concentration could only be correctly estimated with four-way PARAFAC. Finally, the viability of determining heavy-PAHs in natural water samples, without performing tedious sample processing, was demonstrated.

2. Experimental

2.1. Reagents

All experiments were performed with reagents of high-purity grade. BaP, DBA, BbF, BkF, BaA, pyrene (PYR), chrysene (CHRY), fluoranthene (FLT), thiabendazol (TBZ), naphthol (NAP), 1-naphthyl acetic acid (NAA), lomefloxacin (LOME), norfloxacin (NOR), and methyl-β-CD (M-β-CD) were purchased from Sigma-Aldrich (Milwaukee, USA). β-CD and hydroxypropyl-β-CD (HP-β-CD) were acquired from Cyclolab (Budapest, Hungary). Ciprofloxacin (CIPRO) and enrofloxacin (ENRO) were obtained from Fluka (Buchs, Switzerland). Fuberidazol (FBZ) and danofloxacin (DANO) were provided by Riedel-de Haën (Seelze, Germany). Methanol, acetonitrile, acetic acid, sodium acetate, and ferrous ammonium sulfate were obtained from Merck (Darmstadt, Germany). Hydrogen peroxide 30% (w/w) was purchased from Cicarelli (San Lorenzo, Argentina). Stock solutions of all PAHs of about 100 mg L^{-1} were prepared in acetonitrile. From these solutions, 2 mg L^{-1} acetonitrile solutions were obtained. Both diluted hydrogen peroxide and ferrous ammonium sulfate solutions were standardized by titration with potassium permanganate. Ultra pure water was obtained from a Milli-Q system (Waters Millipore). A buffer solution (pH 5; C = 0.1 mol L^{-1}) was prepared from acetic acid and sodium acetate. Due to their high toxicity, PAHs reagents were handled with extreme caution, using gloves and protective clothing.

2.2. Apparatus

Fluorescence spectral measurements were performed on a Varian Cary Eclipse fluorescence spectrophotometer connected to a PC microcomputer via an IEEE 488 (GPIB) serial interface. The Cary Eclipse software was used for data acquisition. Excitation–emission-time data arrays were recorded in the following ranges: excitation, 240–328 nm, each 4 nm, emission, 370–470 nm, each 3.33 nm, and time 0–4.2 min, each 0.42 min. In this work, a scanning speed of 16,000 nm min^{-1} was used, allowing the recording of each EEFM in a time significantly smaller than the time between successive measurements. In other words, the fast scanning recording avoided the loss of data quadrilinearity, as will be demonstrated by the good results obtained with four-way PARAFAC [24]. The cell was thermostated at 20 °C by use of a thermostatic cell holder and a Lauda (Frankfurt, Germany) RM6T thermostatic bath.

2.3. Experimental conditions

Different conclusions have been obtained about the pH effect on Fenton oxidation of organic compounds in water. While some authors reported acid pH values (pH = 3–5) as the most effective ones for this oxidation [25,32], other researchers found that neutral pH is optimum to degrade organic compounds in water [26]. Specifically in the case of BaP, it was observed that the removal efficiency was not significantly changed in the pH range 3.5 to 6 [27], and a pH = 5 given by an acetate/acetic acid (0.01 mol L^{-1}) buffer was here selected.

It was demonstrated that initial concentrations of ferrous ion (catalytic agent) in the range 3–5.5 mg L^{-1} have a positive effect on the oxidation rate [26,27]. In the present work, an initial ferrous ion concentration of 2 mg L^{-1} allowed an appropriate reaction rate, and did

not exceed the limit allowed by the European Economic Community for iron discharged directly into the environment [27].

The effect of hydrogen peroxide concentration was evaluated from 5 to 20 mg L^{-1}. Because higher concentrations of this reagent increase the degradation rate of BaP, a value of 5 mg L^{-1} was selected.

A temperature higher than 30 °C led to an increase in the degradation reaction [27] and, therefore, preliminary experiments were conducted at 10, 15 and 20 °C. Because there were no significant differences between these experiments, all measurements were carried out at 20 °C.

The selected M-β-CD concentration (0.01 mol L^{-1}) was in a large excess with respect to the analytes. This significantly increases the PAHs solubilities, and ensures their highest fluorescence signals.

2.4. Calibration, validation and test sets

A calibration set of 15 samples containing the five analytes was prepared (Table S2, Supplemantary data). Twelve samples of the set corresponded to the concentrations provided by a Plackett-Burman design. Two of the remaining samples were blank solutions, and the last sample contained the five studied PAHs at average levels. The tested concentrations were in the ranges 0–70 ng mL^{-1} for DBA, BbF, and BaA, and 0–45 ng mL^{-1} for BaP and BkF. These ranges were established on the basis of the analysis of the linear fluorescence-concentration range for each PAH.

A validation set was prepared employing concentrations different than those used for calibration and following a random design. Calibration and validation samples were prepared by placing appropriate aliquots of acetonitrile standard solutions in 2.00 mL volumetric

flasks, evaporating the solvent with nitrogen, adding M-β-CD (C_{final} = 0.01 mol L^{-1}), acetic/acetate buffer solution (pH 5) and ultra pure water to the mark.

As will be demonstrated below, some PAHs such as PYR, CHRY and FLT, and certain agrochemicals (FBZ, TBZ, NAP, and 1-NAA) have fluorescence signals overlapping with those of the studied compounds. Therefore, with the purpose of evaluating the method in the presence of these potentially interfering compounds, 10 samples containing random concentrations of the five studied heavy-PAHs and concentrations of these potential interferences were prepared. The interferences were evaluated at the following concentration ranges: 0-300 ng mL^{-1} for NAP, FLT, TBZ, and 1-NAA, 0-200 ng mL^{-1} for PYR and CHRY, 0-50 ng mL^{-1} for FBZ. This set was named as test set No. 1.

The proposed approach also was assessed in the presence of five fluoroquinolones, namely CIPRO, DANO, ENRO, LOME, and NOR (test set No. 2). Fluoroquinolones are antibiotics widely employed in human and veterinarian medicine and they are often found in surface waters. Fluoroquinolones also present overlapping spectra with the analysed PAHs and they were included at concentrations between 200 and 500 ng mL^{-1}.

Both test sets were prepared by placing appropriate aliquots of analytes standard solutions and interferents solutions in 2.00 mL volumetric flasks, evaporating the solvent with nitrogen, adding M-β-CD (C_{final} = 0.01 mol L^{-1}), acetic/acetate buffer solution (pH 5) and ultra pure water to the mark.

2.5. Water samples

Underground, ditch and stream waters were collected in glass bottles with PTFE-lined caps from different regions of our country, and stored at 4 °C until analysis. Because the investigated real samples did not contain the studied PAHs at levels detected by the proposed

strategy (even after pre-concentration), they were first spiked with the analytes and then filtered twice through filter paper to remove suspended solid materials. Although some of these samples contained significant amounts of humic acids and proteic substances as potential fluorescent interferents, the same agrochemicals, PAHs and fluoroquinolones used in the test samples were incorporated in real matrices at different concentrations. With the purpose of covering a wide range of concentrations and evaluating PAHs at sub-part-per-billion levels, a set of water samples was subjected to a solid-phase extraction (SPE) using a C18 extraction membrane (Empore, Supelco, Belleponte, USA) before sample analysis. Previously, the extraction efficiency of about 100% was assured testing different volumes of distilled water solutions of the analytes. The disks were loaded into a 13 mm stainless steel filter syringe kit (Alltech, Deerfield, IL, USA) and placed into a syringe. Prior to sample application, the disk was conditioned with methanol and ultra pure water. Aliquots of 100–500 mL of aqueous samples were passed through the membrane under vacuum pump, with a flow rate of about 30 mL min^{-1}. After elution of the retained organic compounds with 1.5 mL of acetonitrile, the solvent was evaporated by using dry nitrogen and reconstituted with M-β-CD (C_{final} = 0.01 mol L^{-1}) and acetic/acetate buffer solution (pH 5) to a final volume of 2.00 mL. Finally, the EEFM-kinetic (EEFM-K) data were measured for each sample and the PAHs concentrations were estimated using third-order/four-way calibration.

2.6. Analytical measurement

The quartz cell containing the corresponding working solution (calibration, validation or test sample solution) was placed in the spectrofluorimeter at 20 °C prior to signal collection. Then, 10 µL of 2 mg L^{-1} ferrous ammonium sulfate solution followed by 7 µL of 5 mg L^{-1} hydrogen peroxide were added, indicating the start of the fluorescence measurements,

because this latter addition induces the Fenton reaction. Third-order data were then obtained and analyzed with third-order/four-way calibration.

2.7. Chemometric algorithms and software

The theory corresponding to three- and four-way PARAFAC is well documented in the literature [24]. Both a brief description of multivariate calibration with four-way PARAFAC and a short stepwise scheme for the employed external calibration mode are provided in the Supplementary Material. The data were handled using the MATLAB computer environment (MATLAB R2012a), and were implemented using graphical interfaces: MVC2 [28] and MVC3 [29], which are integrated MATLAB toolboxes for second- and third-order calibrations, respectively. They are freely available on the Internet [30,31].

3. Results and discussion

3.1. Fenton degradation of PAHs

Fenton's reagent is a mixture of H_2O_2 and Fe(II) ion, resulting in the generation of strong non-specific oxidant hydroxyl radicals according to the following reaction:

$$Fe^{2+} + H_2O_2 \rightarrow Fe^{3+} + OH^{\bullet} + OH^{-} \quad (1)$$

Hydroxyl radicals can oxidize most organic compounds (RH) by abstraction of protons producing organic radicals ($R^{\bullet}$), which are highly reactive and can be further oxidized [32]:

$$RH + OH^{\bullet} \rightarrow H_2O + R^{\bullet} \rightarrow \text{further oxidation} \quad (2)$$

According to the literature, oxygenated PAHs such as ketones and quinones appear to be important oxidation products during Fenton oxidation of PAHs [33].

As was previously indicated, the Fenton reaction is employed for PAHs chemical degradation in the remediation of water and soils [22,23]. In the latter case, the main objective is to achieve the best efficiency of reaction, which depends on reagent concentrations, pH and temperature [34]. In the present work, the experimental conditions were adjusted in order to: 1) increase the sensitivity of the assay, and 2) carry out the oxidation in a reasonable period of time. Among the investigated PAHs, BaP shows a high ionization potential and is the most susceptible to chemical oxidation [35]. Therefore, optimization of the experimental conditions was carried out to reach a degradation rate of BaP which was slow enough to permit the recording of the kinetic profiles of the other investigated PAHs, without excessively increasing the overall measurement time.

With the purpose of increasing the sensitivity of the fluorescence detection and the solubility of the studied compounds through the formation of inclusion complexes, selected CDs were added to the working solution [36]. The ability of certain CDs to simultaneously coordinate iron ion and hydrophobic organic compounds has been used with the purpose of improving the efficiency of the Fenton reaction [37]. Veignie et al. concluded that Fenton degradation of BaP was strongly dependent on the capacity of the CD to solubilize this PAH [22]. HP-β-CD was the best option, possibly due the formation of an HP-β-CD–BaP–iron ternary complex which allows the generation of hydroxyl radicals in close proximity to BaP and minimizing the HP-β-CD degradation [22]. The formation of a ternary HP-β-CD–phenanthrene–iron complex was also proposed for explaining the effective degradation of the pollutant in the presence of HP-β-CD using an electro-Fenton process [38]. Among the investigated CDs, namely β-CD, HP-β-CD and M-β-CD, the latter one produced a significant increase in the fluorescence intensity of the less fluorescent PAH (e.g. DBA). Besides, the

presence of M-β-CD provided a reasonable compromise between degradation time and EEFMs registering speed. The experimental working conditions in the subsequent experiments are summarized in Table 1.

Near here Table 1

3.2. Third-order EEFM-K data

BaP, DBA, BbF, BkF and BaA present excitation and emission fluorescence spectra in similar wavelength regions, with a significant spectral overlapping and the concomitant problem for their direct and simultaneous spectrofluorimetric determination (Fig. 1A). In fact, when intrinsically unselective signals are employed for analyzing complex samples, the univariate approach is not feasible [10].

Near here Fig. 1

Unavoidably, the situation would be worse with the presence of potential spectral interferences in real samples. Multivariate calibration algorithms provide sensible solutions to the problem of the spectral interfering agents, particularly when high-order instrumental data are available. Because second-order algorithms allow concentrations and spectral profiles of sample components to be extracted directly, the system could be resolved, in principle, employing EEFMs and second-order/three-way calibration (Table S1).

However, for complex systems with serious spectral interference a suitable option is to employ third-order/four-way calibration [39]. This type of calibration includes the second-order advantage, because this property is intrinsic to all data of at least second-order [12], and provides an enhanced resolving power with a higher sensitivity [39]. Sensitivity is increased

because the measurement of redundant data tends to decrease the relative impact of the noise in the signal. Selectivity does also increase because each new instrumental mode added to the data contributes positively to the overall selectivity.

Therefore, an additional mode (i.e. kinetic) was measured by subjecting the studied system to the Fenton reaction under the previously selected experimental conditions (see above). Although the kinetic behavior of BaP towards the Fenton reaction is markedly unique (Fig. 1A), each PAH has its characteristic decay rate, adding selectivity to the component resolution.

In a first stage, for building a third-order/four-way calibration model, EEFM-K data were measured for calibration and validation samples, which only contained the five analytes. Significantly more complex samples including potential interferences were then studied. For clarity, the two evaluated test sets, with different degrees of difficulty, were numbered as test set No. 1 and test set No. 2.

Several algorithms exist for the analysis of four-way data. However, if the set of EEFMs-K can be arranged as a four-way array complying with the quadrilinearity condition [10], the algorithm of choice is the popular PARAFAC, which in this specific case is called four-way PARAFAC [10].

3.2.1. Validation samples

The method was validated through the processing of validation samples and the corresponding recovery analysis and figures of merit calculation.

Fig. 2A shows the excitation-emission fluorescence contour plots as a function of different reaction times for a typical validation sample, when the studied PAHs react with Fenton's reagent under the selected conditions. As expected, the fluorescence intensity of the system considerably decreases as a function of reaction time.

Near here Fig. 2

Four-way PARAFAC was initialized by singular value decomposition (SVD) vectors, and scores and loadings were restricted to be non-negative during the alternating least-squares fitting phase. The number of fluorescent components in the four-way arrays was carried out through both the analysis of PARAFAC residuals [24] and the consideration of the spectral profiles produced by the addition of subsequent components. Thus, if the addition of a new component generated repeated profiles, suggesting overfitting, the new component was discarded and the previous number of components was selected. Five components of PARAFAC, corresponding to the five presently studied analytes, were required to describe the variability in these data arrays, providing suitable emission, excitation and kinetic profiles (Fig. 1B), and good prediction results [Fig. 3A (left)].

Near here Fig. 3

The quality of the four-way PARAFAC recovered profiles was evaluated using the criterion of similarity which involves a comparison through the similarity coefficient (R) between the reference (Fig. 1A) and retrieved profiles (Fig. 1B) [40]. The values of R found for BaP, DBA, BbF, BkF and BaA were, respectively, 0.9948, 0.9928, 0.9874, 0.9990, 0.9972 for the emission profiles, 0.9938, 0.9937, 0.9938, 0.9979, 0.9978 for the excitation profiles, and 0.9973, 0.9996, 0.9999, 0.9937, 0.9842 for the kinetic profiles. These values corroborate the excellent quality of the four-way PARAFAC results. Moreover, Fig. 1C and Fig. 1D show the score profiles for set composed of a typical validation sample and all calibration samples. A good correlation exists between nominal analyte concentrations (Fig. 1C) and four-way PARAFAC component scores (Fig. 1D).

The analysis of these results in relation to those obtained when second-order EEFMs data of the same validation samples are processed with three-way PARAFAC [Fig. 3A (medium)] suggests that both predictions are good, although a larger dispersion is verified in the second case. The statistical comparison between both types of calibrations was carried out by the EJCR (elliptical joint confidence region) test for the slope and intercept of the found vs nominal concentrations plot [41]. Since various analytes were simultaneously determined, the joint confidence interval test was calculated considering the experimental data corresponding to all analytes, following literature suggestions [42]. When the EJCR test is only applied to single-analyte data, the estimated variance might be overestimated, making the joint confidence region too large and increasing the probability of not detecting the presence of bias [42]. In our case, the obtained ellipses (Fig. 3A) include the theoretically expected values of slope = 1 and intercept = 0, indicating the accuracy of both methodologies [41].

The statistical results of Table 2 show that both the root-mean square errors (RMSEs) and the relative errors of prediction (REPs), computed with respect to the mean calibration concentration of each analyte, are slightly lower in third-order/four-way calibration, with better sensitivity values. The difference in the selectivity is more marked in the case of BaP, with its distinctive kinetic mode.

Near here Table 2

Finally, the favorable influence of M-β-CD on the fluorescence intensity of the analytes and the benefits of the third-order are proven in the good limits of detection (LODs) and limits of quantitation (LOQs) obtained with the proposed method. These limits were estimated using the critical expressions recommended by IUPAC for the detection

capabilities, which take into account the so-called Type 1 and 2 errors (false detects and false non-detects respectively) [11,43]:

$$\mathrm{LOD} = 3.3\,(\mathrm{SEN}^{-2}\sigma_x^2 + h_0\mathrm{SEN}^{-2}\sigma_x^2 + h_0\sigma_{y\mathrm{cal}}^2)^{1/2} \quad (3)$$

where the factor 3.3 is given by $(2\times t_{0.05,\infty})$, SEN is the sensitivity, σ_x^2 is the instrumental variance, $\sigma_{y\mathrm{cal}}^2$ is the calibration concentration variance, and h_0 is the leverage for a blank sample [11]. The limit of quatitation is defined as [11]:

$$\mathrm{LOQ} = 3\ \mathrm{LOD} \quad (4)$$

3.2.2. Test set No. 1

Test samples containing additional constituents to those present in calibration and validation are frequently employed in multiway calibration to probe its ability to distinguish the presence of foreign compounds. The analysis of this type of samples allows one to appreciate the capacity of multiway calibration to overcome the ubiquitous problem of the potential presence of interfering species in the analyzed matrices.

Among different priority and common pollutants, CHRY, PYR, and FLT, and the agrochemicals TBZ, FBZ, 1-NAA and NAP have fluorescence signals overlapped in different degree with those of the studied analytes (Figs. 4A-C). Besides, if relatively high levels of potential interferences are added, the analyte signals are completely masked, stressing the importance of appealing to the advantage second-order advantage for resolving the system.

Near here Fig. 4

Consequently, ten test samples containing the analytes and different concentration ratios of the above mentioned compounds were prepared according to the discussion

presented in the experimental section and were evaluated with both four- and three-way PARAFAC.

Figure 2B shows the evolution of the EEFMs during Fenton degradation of a typical sample containing additional PAHs and agrochemicals selected as potential interferences. In this figure, the challenge in resolving the system is apparent since the fluorescence of the analytes cannot be distinguished from that of the foreign compounds.

The number of total components required by four-way PARAFAC in samples of test set No. 1 varied between six and nine, and was established in the same way that in validation samples. It is usual that when several unexpected components occur in test samples, the profiles retrieved by four-way PARAFAC may not completely resemble those of the real interferences [44].

Near here Fig. 5

As is apparent in Fig. 5A, while the profiles of each analyte are correctly recovered by four-way PARAFAC, those for some interferents are retrieved as a linear combination of the pure component profiles shown in Figs. 4B and 4C. This fact did not influence neither the successful prediction of the constituent concentrations in the investigated samples [Fig. 3B (left)] nor the good statistical values (Table 2). The presence of foreign compounds in the samples decreases the selectivity values, and LODs of DBA and BbF are slightly larger than those for validation samples. In the former case, this fact can be ascribed to the similarity between the excitation spectra of DBA and FLT, and in the latter one, it is clear that the emission profile of BbF is very similar to those of FLT and NAA (Fig. 4).

Although the quantification of the analytes carried out through EEFMs and three-way PARAFAC rendered accurate results [Fig. 3B (medium)], a lower precision in the obtained

recoveries is verified. The differences between both types of calibrations are more evident in the size of the corresponding ellipses of the EJCR test [Fig. 3B (right)] and in the statistical summary presented in Table 2. As a partial conclusion, we can say that the addition of a third mode to the system (the kinetic one) had a positive impact on the resolution of the system.

3.2.3. Test set No. 2

With the purpose of evaluating the ability of four-way PARAFAC to solve systems that are difficult to be elucidated by three-way PARAFAC, a new test set of samples (test set No. 2) containing the studied analytes and fluoroquinolones was processed. The emission fluorescence spectra of the five selected fluoroquinolones are very similar to each other (Fig. 4D) and, in turn, are very similar to that of BbF (Fig. 4A). Third-order/four way calibration could, in principle, overcome this situation, provided the interferent profiles in the additional mode are different from that of the analyte.

Fig. 2C displays the Fenton degradation of a sample of test set No. 2 through the corresponding EEFMs contour plots at different evolution times. The number of four-way PARAFAC components in these samples was 6, suggesting that the five fluoroquinolones incorporated as interferences only provide a single additional PARAFAC component. The profiles retrieved by four-way PARAFAC for this additional component are shown in Fig. 5B. While a spectral similarity with the emission of BbF is verified, the profiles of this additional component in both excitation and kinetic modes, which are the ones responsible for the selectivity towards BbF, are clearly distinguished.

Fig. 3C (left) shows the good four-way PARAFAC results obtained for all predicted PAH concentrations, and the statistical study of the results (Table 2) indicates that, in general, neither the sensitivity nor the selectivity of the method is seriously affected by the presence of

fluoroquinolones when applying four-way PARAFAC. Although the LOD for BbF is larger than the one in validation samples, it remains at a satisfactory part-per-billion level.

In the case of three-way PARAFAC, the second-order advantage may be lost when a non-calibrated constituent has a very similar profile to that of the analyte in one of the modes, even when there is selectivity in both modes among the calibrated constituents. This phenomenon occurs in the present system regarding BbF in test set No. 2. As a consequence, the concentration of BbF cannot be correctly predicted in test set. Indeed, in comparing four-way PARAFAC predictions with those obtained with three-way PARAFAC through the EEFMs processing [Fig. 3C (medium), Table 2], one may conclude that the latter calibration rendered relatively disperse recovery values for BaP, DBA, BkF and BaA, and inaccurate values for BbF, corroborating the inability of this algorithm to perform the successful decomposition of the second-order data for BbF when interferences with a very similar spectra are present. This conclusion can also be obtained from the large size of the ellipse obtained when the EJCR analysis is applied [Fig. 3C (right)].

Several reports suggested that third-order data do not show additional properties, beyond the second-order advantage (e.g. determination of mixture components in complex samples containing uncalibrated interferences) [12–18]. However, Kang et al. recently resolved a system with spectral collinearity through four-way EEFMs–pH arrays, and proposed that the resolution was achieved thanks to the third-order advantage [19]. In the present example, the high degree of collinearity between one of the analytes and an interferent emphasizes the need for an additional mode to solve the system, and this may confirm the presence of a real third-order advantage.

3.2.4. Real samples

In view of the above results, third-order/four-way calibration was selected for the subsequent analysis of real water samples. Due to the existence of many sources of PAHs (petroleum spill during transportation, urban and rural runoff, refining oil-well drilling, wastewater of industrial activities, etc), different levels of these pollutants could be found in natural waters [45]. Total content of PAHs in surface and groundwater can vary from a few parts-per-trillion to parts-per-billion in contaminated areas [46,47]. It must be considered that, for drinking water, the United States Environmental Protection Agency (US EPA) established as the maximum contaminant levels (MCLs) the following values: 0.2 ng mL^{-1} for BaP, BbF, and BkF, 0.1 ng mL^{-1} for BaA, and 0.3 ng mL^{-1} for DBA [48].

Because the analyzed water samples did not contain the studied PAHs, they were spiked with all analytes and also with the potential interferences, and a recovery study was carried out. A wide range of concentrations was covered, evaluating water samples with and without a pre-concentration treatment, and the results are shown in Table 3.

Near here Table 3

Due to the different PAH contents in both types of samples, the statistical EJCR test for slopes and intercepts of the found vs nominal concentration plots was separately applied to samples with and without SPE. The obtained ellipses (Fig. 6) support that there are no statistical differences between found and nominal concentrations, suggesting that neither the added foreign compounds nor other species which are present in the studied matrices have a significant interference in our analysis.

Near here Fig. 6

4. Conclusions

The present research reports on a new application of three-order/four-way excitation-emission fluorescence-kinetic data, intended at the quantitative determination of five heavy-polycyclic aromatic hydrocarbons of concern in environmental samples. The approach based on the measurement of excitation-emission fluorescence matrices of the analytes during their Fenton degradation provides simple and accurate quantitative analysis for the determination of the PAH mixtures without other PAHs, agrochemicals and fluoroquinolones assayed as interferences.

In comparison with second-order calibration, the main advantage of this methodology, applied to samples where only analytes are present, is a higher sensitivity. However, in more complex samples containing potential interferences, the superiority in selectivity and precision of third-order/four-way calibration is evident, providing notably better figures of merit. Specifically, fluoroquinolones tested as potential interferents were challenging due to their spectral overlap with the BbF emission band, but their presence posed no problems to the applied chemometric calibration. This may be taken as supporting the existence of a third-order advantage. On the other hand, the fact that Fenton reaction also degrades organic compounds (e.g. organic matter in real water samples of unknown composition) significantly reduces potential interference and simplifies chemometric analysis.

In conclusion, the proposed method is sensitive (limits of detection below part-per-billion levels), selective (the five PAHs are simultaneously determined in the presence of interferences), involves low experimental time (about 4 min per sample), the computer implementation is very simple and, because the volumes of organic solvents employed are minimal, the method is environmentally friendly.

Acknowledgments

The authors are grateful to the Consejo Nacional de Investigaciones Científicas y Técnicas (CONICET, Project PIP 0163), Universidad Nacional de Rosario (Project BIO 237), and Agencia Nacional de Promoción Científica y Tecnológica (ANPCyT, PICT 2013-0136) for financially supporting this work. M.D.C thanks ANPCyT for a doctoral fellowship.

References

[1] T. Wenzl, R. Simon, J. Kleiner, E. Anklam, Analytical methods for polycyclic aromatic hydrocarbons (PAHs) in food and the environment needed for new food legislation in the European Union, Trends Anal. Chem. 25 (2006) 716–725.

[2] IARC monographs on the evaluation of carcinogenic risks to humans. http://monographs.iarc.fr/ENG/Classification/ (accessed November 2016).

[3] W.B.Wilson, B. Alfarhani, A.F.T. Moore, C. Bisson, S.A. Wise, A.D. Campiglia, Determination of high-molecular weight polycyclic aromatic hydrocarbons in high performance liquid chromatography fractions of coal tar standard reference material 1597a via solid-phase nanoextraction and laser-excited time-resolved Shpol'skii spectroscopy, Talanta 148 (2016) 444–453.

[4] H.I. Abdel Shafy, M.S.M. Mansour, A review on polycyclic aromatic hydrocarbons: source, environmental impact, effect on human health and remediation, Egypt. J. Petrol. 25 (2016) 107–123.

[5] S.A. Bortolato, J.A. Arancibia, G.M. Escandar, Chemometrics-assisted excitation-emission fluorescence spectroscopy on nylon membranes. Simultaneous determination of benzo[a]pyrene and dibenz[a,h]anthracene at parts-per-trillion levels in the presence of the remaining EPA PAH priority pollutants as interferences, Anal. Chem. 80 (2008) 8276–8286.

[6] S.A. Bortolato, J.A. Arancibia, G.M. Escandar, Non-trilinear chromatographic time retention-fluorescence emission data coupled to chemometric algorithms for the simultaneous determination of 10 polycyclic aromatic hydrocarbons in the presence of interferences, Anal. Chem. 81 (2009) 8074–8084.

[7] S.A. Bortolato, J.A. Arancibia, G.M. Escandar, Chemometrics-assisted fluorimetry for the rapid and selective determination of heavy polycyclic aromatic hydrocarbons in contaminated river waters and activated sludges, Environ. Sci. Technol. 45 (2011) 1513–1520.

[8] A. Cañas, P. Richter, G.M. Escandar, Chemometrics-assisted excitation–emission fluorescence spectroscopy on nylon-attached rotating disks. Simultaneous determination of polycyclic aromatic hydrocarbons in the presence of interferences, Anal. Chim. Acta 852 (2014) 105–111.

[9] G.M. Escandar, H.C. Goicoechea, A. Muñoz de la Peña, A.C. Olivieri, Second- and higher-order data generation and calibration: A tutorial, Anal. Chim. Acta 806 (2014) 8–26.

[10] A.C. Olivieri, G.M. Escandar, Practical three-way calibration, Elsevier, Waltham, USA, 2014.

[11] A.C. Olivieri, Analytical figures of merit: from univariate to multiway calibration, Chem. Rev. 114 (2014) 5358−5378.

[12] K.S. Booksh, B.R. Kowalski, Theory of Analytical Chemistry, Anal. Chem. 66 (1994) 782A–791A.

[13] A. Jiménez-Girón, I. Durán-Merás, A. Espinosa-Mansilla, A. Muñoz de la Peña, F. Cañada-Cañada, A.C. Olivieri, On line photochemically induced excitation-emission-kinetic four way data: analytical application for the determination of folic acid and its

two main metabolites in serum by U-PLS and N-PLS/residual trilinearization (RTL) calibration, Anal. Chim. Acta 622 (2008) 94–103.

[14] A.C. Olivieri, J.A. Arancibia, A. Muñoz de la Peña, I. Durán-Merás, A. Espinosa-Mansilla, Second-order advantage achieved with four-way fluorescence excitation-emission-kinetic data processed by parallel factor analysis and trilinear least-squares. Determination of methotrexate and leucovorin in human urine, Anal. Chem. 76 (2004) 5657–5666.

[15] P.C. Damiani, I. Durán-Merás, A. García-Reiriz, A. Jiménez-Girón, A. Muñoz de la Peña, A.C. Olivieri. Multiway partial least-squares coupled to residual trilinearization: a genuine multidimensional tool for the study of third-order data. Simultaneous analysis of procaine and its metabolite p-aminobenzoic acid in equine serum, Anal. Chem. 79 (2007) 6949–6958.

[16] X.D. Qing, H.L. Wu, X.F. Yan, Y. Li, L.Q. Ouyang, C.C. Nie, R.Q. Yu, Development of a novel alternating quadrilinear decomposition algorithm for the kinetic analysis of four-way room temperature phosphorescence data, Chemom. Intell. Lab. Syst. 132 (2014) 8–17.

[17] A. García-Reiriz, P.C. Damiani, A.C. Olivieri, F. Cañada-Cañada, A. Muñoz de la Peña, Nonlinear four-way kinetic-excitation-emission fluorescence data processed by a variant of parallel factor analysis and by a neural network model achieving the second-order advantage: malonaldehyde determination in olive oil samples, Anal. Chem. 80 (2008) 7248–7256.

[18] R.M. Maggio, P.C. Damiani, A.C. Olivieri, Four-way kinetic-excitation-emission fluorescence data processed by multi-way algorithms. Determination of carbaryl and 1-

naphthol in water samples in the presence of fluorescent interferents, Anal. Chim. Acta 677 (2010) 97–107.

[19] C. Kang, H.L. Wu, L.X. Xie, S.X. Xiang, R.Q. Yu, Direct quantitative analysis of aromatic aminoacids in human plasma by four-way calibration using intrinsic fluorescence: exploration of third-order advantages, Talanta 122 (2014) 293–301.

[20] N. Rodríguez, M.C. Ortiz, L.A. Sarabia, Fluorescence quantification of tetracycline in the presence of quenching matrix effect by means of a four-way model, Talanta 77 (2009) 1129–1136.

[21] H.C. Goicoechea, S. Yu, A.C. Olivieri, A.D. Campiglia, Four-way data coupled to parallel factor model applied to environmental analysis: determination of 2,3,7,8-tetrachloro-dibenzo-para-dioxin in highly contaminated waters by solid-liquid extraction laser-excited time-resolved Shpol'skii spectroscopy, Anal. Chem. 77 (2005) 2608–2616.

[22] E. Veignie, C. Rafin, D. Landy, S. Fourmentin, G. Surpateanu, Fenton degradation assisted by cyclodextrins of a high molecular weight polycyclic aromatic hydrocarbon benzo[a]pyrene. J. Hazard. Mater. 168 (2009) 1296–1301.

[23] F.J. Rivas, Polycyclic aromatic hydrocarbons sorbed on soils: a short review of chemical oxidation based treatments, J. Hazard. Mater. 138 (2006) 234–251.

[24] R. Bro, PARAFAC. Tutorial and applications, Chemometr. Intell. Lab. Syst. 38 (1997) 149–171.

[25] D.L. Sedlak, A.W. Andren, Oxidation of chlorobenzene with Fenton's reagent. Environ. Sci. Technol. 25 (1991) 777–782.

[26] F.J. Beltrán, M. González, F.J. Rivas, P. Alvarez, Fenton reagent advanced oxidation of polynuclear aromatic hydrocarbons in water, Water Air Soil Poll. 105 (1998) 685–700.

[27] V. Homem, Z. Dias, L. Santos, A. Alves, Preliminary feasibility study of benzo(a)pyrene oxidative degradation by Fenton treatment, J. Environ. Public Health 2009 (2009) article ID 149034, 6 pages, doi:10.1155/2009/149034.

[28] A.C. Olivieri, H.L. Wu, R.Q. Yu, MVC2: a MATLAB graphical interface toolbox for second-order multivariate calibration, Chemom. Intell. Lab. Syst. 96 (2009) 246–251.

[29] A.C. Olivieri, H.L. Wu, R.Q. Yu, MVC3: A MATLAB graphical interface toolbox for third-order multivariate calibration, Chemom. Intell. Lab. Syst. 116 (2012) 9–16.

[30] www.iquir-conicet.gov.ar/descargas/mvc2.rar (accessed November 2016).

[31] www.iquir-conicet.gov.ar/descargas/mvc3.rar (accessed November 2016).

[32] E. Neyens, J. Baeyens. A review of classic Fenton's peroxidation as an advanced oxidation technique, J. Hazard. Mater. B98 (2003) 33–50.

[33] S. Lundstedt, Y. Persson, L. Öberg, Transformation of PAHs during ethanol-Fenton treatment of an aged gasworks' soil, Chemosphere 65 (2006) 1288–1294.

[34] J. Yoon, Y. Lee, S. Kim, Investigation of the reaction pathway of OH radicals produced by Fenton oxidation in the conditions of wastewater treatment, Water Sci. Technol. 44 (5) (2001) 15–21.

[35] S. Jonsson, Y. Persson, S. Frankki, B. van Bavel, S. Lundstedt, P. Haglund, M. Tysklind, Degradation of polycyclic aromatic hydrocarbons (PAHs) in contaminated soils by Fenton's reagent: A multivariate evaluation of the importance of soil characteristics and PAH properties, J. Hazard. Mater. 149 (2007) 86–96.

[36] J. Szejtli, Introduction and general overview of cyclodextrin chemistry, Chem. Rev. 98 (1998) 1743–1753.

[37] M.E. Lindsey, G. Xu, J. Lu, M.A. Tarr, Enhanced Fenton degradation of hydrophobic organics by simultaneous iron and pollutant complexation with cyclodextrins, Sci. Total Environ. 307 (2003) 215–229.

[38] E. Mousset, N. Oturan, E.D. van Hullebusch, G. Guibaud, G. Esposito, M.A. Oturan, Influence of solubilizing agents (cyclodextrin or surfactant) on phenanthrene degradation by electro-Fenton process e Study of soil washing recycling possibilities and environmental impact, Water Res. 48 (2014) 306–316.

[39] H.L. Wu, C. Kang, Y. Li, R.Q. Yu, Practical analytical applications of multiway calibration methods based on alternating multilinear decomposition, in A. Muñoz de la Peña, H.C. Goicoechea, G.M. Escandar, A.C. Olivieri (Eds.), Data handling in science and technology, Fundamentals and analytical applications of multiway calibration, Amsterdam, Elsevier, 2015, vol. 29, ch. 4.

[40] V. Gómez, M. Miró, M.P. Callao, V. Cerdá, Coupling of sequential injection chromatography with multivariate curve resolution-alternating least-squares for enhancement of peak capacity, Anal. Chem. 79 (2007) 7767–7774.

[41] A.G. González, M.A. Herrador, A.G. Asuero, Intra-laboratory testing of method accuracy from recovery assays, Talanta 48 (1999) 729–736.

[42] A. Martínez, J. Riu, O. Busto, J. Guasch, F.X. Rius, Validation of bias in multianalyte determination methods. Application to RP-HPLC derivatizing methodologies, Anal. Chim. Acta 406 (2000) 257–278.

[43] L. A. Currie, Anal. Chim. Acta 391 (1999) 127–134.

[44] A. Smilde, R. Bro, P. Geladi, Multi-way analysis with applications in the chemical sciences, John Wiley & Sons Ltd, Hoboken, NJ, 2004.

[45] D. Mares Brum, R.J. Cassella, A.D. Pereira Netto, Multivariate optimization of a liquid–liquid extraction of the EPA-PAHs from natural contaminated waters prior to determination by liquid chromatography with fluorescence detection, Talanta 74 (2008) 1392–1399.

[46] Md.J. Alam, D. Yuan, Y.J. Jiang, Y. Sun, Y. Li, X. Xu, Sources and transports of polycyclic aromatic hydrocarbons in the Nanshan Underground River, China, Environ. Earth Sci. 71 (2014) 1967–1976.

[47] R. Sarria-Villa, W. Ocampo-Duque, M. Páez, M. Schuhmacher, Presence of PAHs in water and sediments of the Colombian Cauca River during heavy rain episodes, and implications for risk assessment, Sci. Total Environ. 540 (2016) 455–465.

[48] https://www.atsdr.cdc.gov/csem/csem.asp?csem=13&po=8 (accessed November 2016).

Table 1
Working conditions.

	Values/reagents
pH	5, acetate/acetic acid buffer (0.01 mol L^{-1})
Fe(II) ion concentration (mg L^{-1})	2
H_2O_2 concentration (mg L^{-1})	5
Temperature (°C)	20
M-β-CD concentration (mol L^{-1})	0.01

Table 2
Statistical results for the studied PAHs in validation samples employing third-order EEFM-K and second-order EEFM data.

	EEFM-K data					EEFM data				
Validation set	BaP	DBA	BbF	BkF	BaA	BaP	DBA	BbF	BkF	BaA
RMSEP/ng mL^{-1}	3.1	4.1	3.5	1.4	2.4	4.0	5.9	5.4	1.5	2.8
REP/%	9	11	10	7	7	11	17	15	8	8
Sensitivity/FU ng^{-1} mL	34	27	29	120	70	19	8.4	9.4	37	21
γ/ng^{-1} mL	16	12	14	55	33	10	4.7	5.2	21	12
Selectivity	0.73	0.81	0.66	0.60	0.77	0.58	0.82	0.66	0.54	0.66
LOD/ng mL^{-1}	0.4	0.4	0.4	0.3	0.3	0.5	0.8	0.7	0.3	0.5
LOQ/ng mL^{-1}	1.1	1.3	1.2	0.9	1.0	1.4	2.5	2.2	1.0	1.4
Test set No. 1										
RMSEP/ng mL^{-1}	4.0	3.9	2.9	2.0	3.5	4.1	5.6	4.8	2.7	5.6
REP/%	11	11	8	10	10	12	17	14	13	16
Sensitivity/FU ng^{-1} mL	32	11	7	85	29	10	2.9	0.5	26	9.3
γ/ng^{-1} mL	3.3	1.1	2.8	8.8	3	1.7	0.5	0.04	4.3	1.5
Selectivity	0.61	0.31	0.14	0.37	0.34	0.31	0.28	0.20	0.32	0.30
LOD/ng mL^{-1}	1.1	3.2	3.0	0.5	1.2	2.1	7.5	15	0.9	2.4
LOQ/ng mL^{-1}	3.4	9.7	9.0	1.5	3.7	6.5	23	45	2.7	7.1
Test set No. 2										
RMSEP/ng mL^{-1}	2.9	2.9	1.4	3.5	4.1	3.8	7.1	[a]	3.6	4.3
REP/%	8	8	4	17	11	11	20	[a]	18	12
Sensitivity/FU ng^{-1} mL	24	19	3	68	32	8.2	2.3	[a]	12	4.4
γ/ng^{-1} mL	5.3	4.3	0.7	15	7.1	2.2	0.6	[a]	3.2	1.2
Selectivity	0.51	0.55	0.08	0.35	0.35	0.25	0.22	[a]	0.19	0.14
LOD/ng mL^{-1}	0.7	0.9	5.0	0.4	0.6	1.7	5.9	[a]	1.2	3.1
LOQ/ng mL^{-1}	2.2	2.7	16	1.1	1.8	5.1	18	[a]	3.5	9.5

RMSEP, root mean-square error of prediction; REP, relative error of prediction; FU, fluorescence units; γ, analytical sensitivity; LOD, limit of detection; LOQ, limit of quantification. Sensitivity, selectivity, LOD and LOQ were calculated according to ref. [11].

Table 3
Recovery study for the five studied PAHs in added water samples in the presence of potential interferences using three-order/four-way calibration.[a]

	BaP		DBA		BbF		BkF		BaA	
	Taken	Found	Taken	Found	Taken	Found	Taken	Found	Taken	Found
Without SPE										
Water I	10.0	9.5 (95)	12.9	10.6 (82)	10.0	10.4 (104)	11.9	9.0 (76)	14.3	14.1 (99)
	15.0	12.0 (80)	18.8	18.3 (97)	14.9	14.3 (96)	14.9	12.0 (81)	11.9	11.7 (98)
Water II	21.0	17.4 (83)	21.8	24.1 (110)	31.7	29.0 (91)	8.9	9.4 (106)	13.0	15.6 (120)
	17.0	17.5 (103)	27.8	27.8 (100)	20.0	24.6 (123)	16.9	15.0 (89)	9.9	8.9 (90)
Water III	6.0	5.6 (93)	9.0	11.1 (123)	0	0.8 (--)	5.0	5.8 (116)	46.1	50.6 (110)
	4.8	4.2 (88)	8.0	8.4 (105)	44.5	43.6 (98)	36.0	30.0 (83)	43.0	37.0 (86)
With SPE[b]										
Water II[c]	0.150	0.155 (103)	0.00	0.020 (--)	0.269	0.307 (114)	0.230	0.227 (99)	0.198	0.190 (96)
Water II[d]	0.029	0.024 (83)	0.029	0.020 (69)	0.060	0.072 (120)	0.048	0.056 (116)	0.040	0.050 (125)
Water III[c]	0.071	0.064 (90)	0.067	0.055 (82)	0.076	0.082 (107)	0.069	0.058 (84)	0.050	0.063 (126)
Water III[d]	0.050	0.040 (80)	0.050	0.060 (120)	0.119	0.097 (82)	0.080	0.073 (91)	0.087	0.083 (95)
Water IV[c]	0.087	0.085 (98)	0.084	0.099 (117)	0.100	0.119 (119)	0.095	0.090 (95)	0.090	0.078 (87)
Water IV[d]	0.072	0.060 (83)	0.076	0.058 (76)	0.079	0.078 (99)	0.068	0.081 (119)	0.060	0.042 (70)
Water V[c]	0.194	0.154 (79)	0.209	0.201 (96)	0.175	0.163 (93)	0.149	0.133 (89)	0.067	0.065 (97)
Water V[e]	0.169	0.133 (79)	0.183	0.223 (122)	0.169	0.165 (98)	0.250	0.236 (94)	0.090	0.063 (70)

[a] Water I: ditch water from Funes city (Santa Fe, Argentina). Water II: underground water from Funes city (Santa Fe, Argentina). Water III: water from Ludueña stream (Santa Fe, Argentina), Water IV: underground water from Santa Rosa city (La Pampa, Argentina). Water V: underground water from Venado Tuerto city (Santa Fe, Argentina). Concentrations are given in ng mL^{-1} and recoveries (between parentheses) are given in percentage. The total concentrations of added interferents (see text) were in the range 100–1000 ng mL^{-1}.
[b] The values refer to water samples before SPE.
[c] Volume of treated water = 200 mL.
[d] Volume of treated water = 500 mL.
[e] Volume of treated water = 100 mL.

Figure captions

Fig. 1. (A) Experimental emission (top), excitation (medium) and kinetic (bottom) profiles recorded during Fenton decomposition of BaP (violet), DBA (dark yellow), BbF (orange), BkF (black), and BaA (green) at pH 5 and in the presence of M-β-CD. (B) Profiles retrieved by four-way PARAFAC after processing a validation sample. Insets in the kinetic plots show the decay curves in a restricted scale to better visualize them. (C) Concentrations of all components in the sample set composed of a validation sample (first left) and the subsequent calibration samples. (D) PARAFAC scores for all components in the processed samples. All intensities are normalized to unit length.

Fig. 2. Evolution of the excitation-emission fluorescence contour plots during Fenton degradation under our experimental conditions for a validation sample (A), a sample of test set No. 1 (B), and a sample of test set No. 2, measured at the following starting times: (1) 0, (2) 0.42, (3) 1.67 and (4) 3.75 min.

Fig. 3. (A) Plots for four-way PARAFAC (left) and three-way PARAFAC (medium) predicted concentrations as a function of the nominal values of the five studied PAHs in validation samples and elliptical joint regions at 95% confidence level (right) for slope and intercept of the regression of four-way PARAFAC (solid line) and three-way PARAFAC (dashed line) results. Plots for the same algorithms applied to samples of test set No. 1 (B), and test set No. 2 (C). Red triangles in C (left and medium) show prediction for BbF (see text). Red starts in the ellipses profiles mark theoretical (intercept = 0, slope = 1) points.

Fig. 4. Normalized excitation and emission fluorescence spectra in the presence of 0.01 mol L^{-1} M-β-CD for the studied analytes (A), selected PAHs (B), agrochemicals (C) and fluoroquinolones (D), as indicated.

Fig. 5. Profiles retrieved by four-way PARAFAC after processing a typical sample of test set No. 1 (A), and a typical sample of test set No. 2 (B). Violet, dark yellow, orange, black and green lines indicate the signals ascribed to BaP, DBA, BbF, BkF, and BaA, respectively. Those profiles that do not correspond to the analytes are indicated in gray. Insets in the kinetic plots show the decay curves in a restricted scale to better visualize them. All intensities are normalized to unit length.

Fig. 6. Plots for four-way PARAFAC predicted concentrations as a function of the nominal values of the five studied PAHs in real water samples in the presence of potential interferences, and elliptical joint regions (at 95% confidence level) for the slope and intercept of the regression of the data. Stars mark the theoretical (intercept = 0, slope = 1) points.

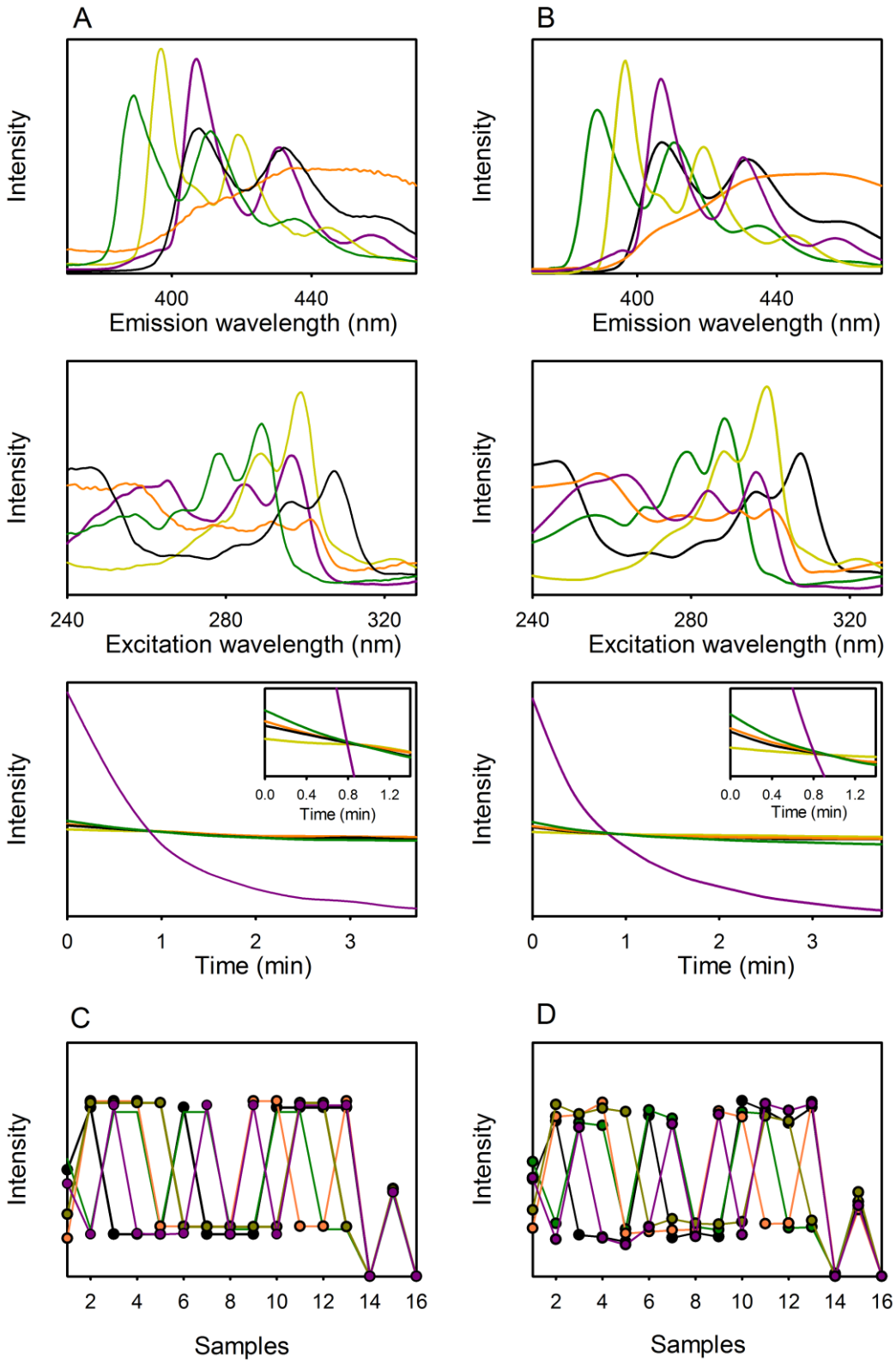
A
B
Intensity
400
440
Emission wavelength (nm)
240
280
320
Excitation wavelength (nm)
0.0
0.4
0.8
1.2
Time (min)
0
1
2
3
C
D
2
4
6
8
10
12
14
16
Samples

Figure 1

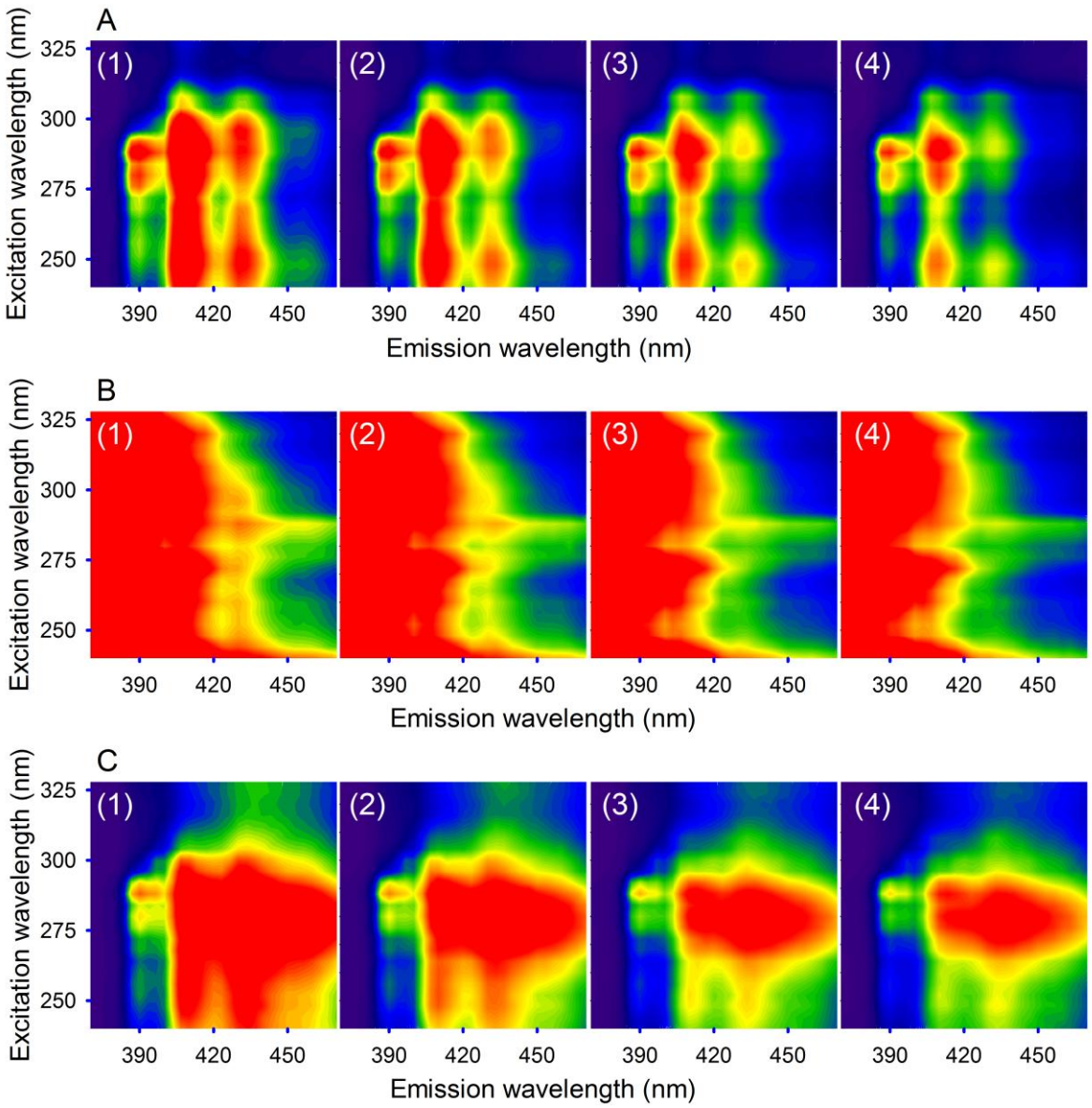
A
B
C
(1)
(2)
(3)
(4)
Excitation wavelength (nm)
325
300
275
250
390
420
450
Emission wavelength (nm)

Figure 2

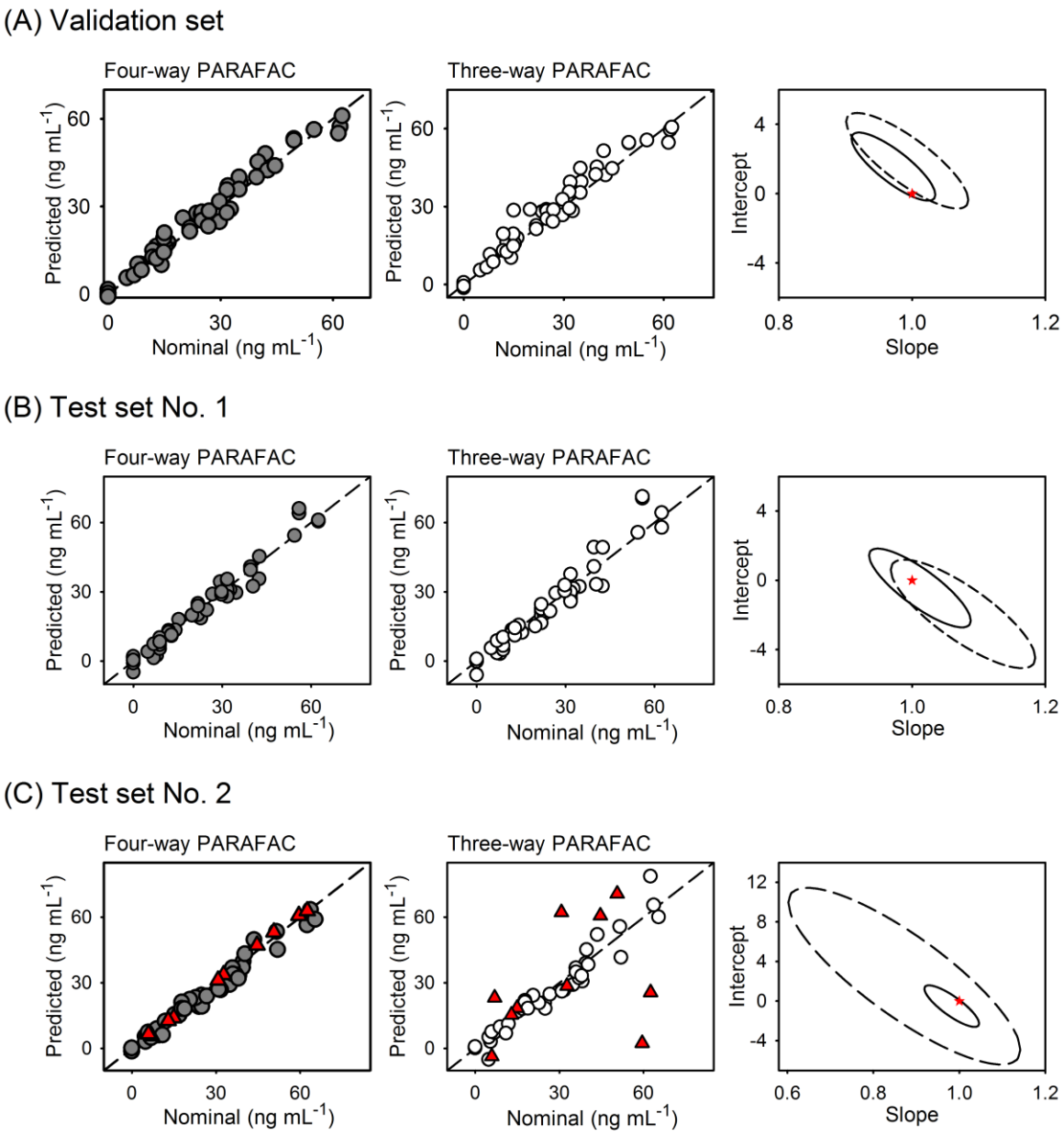
(A) Validation set
Four-way PARAFAC
Three-way PARAFAC
Predicted (ng mL-1)
Nominal (ng mL-1)
Intercept
Slope
(B) Test set No. 1
Four-way PARAFAC
Three-way PARAFAC
Predicted (ng mL-1)
Nominal (ng mL-1)
Intercept
Slope
(C) Test set No. 2
Four-way PARAFAC
Three-way PARAFAC
Predicted (ng mL-1)
Nominal (ng mL-1)
Intercept
Slope

Figure 3

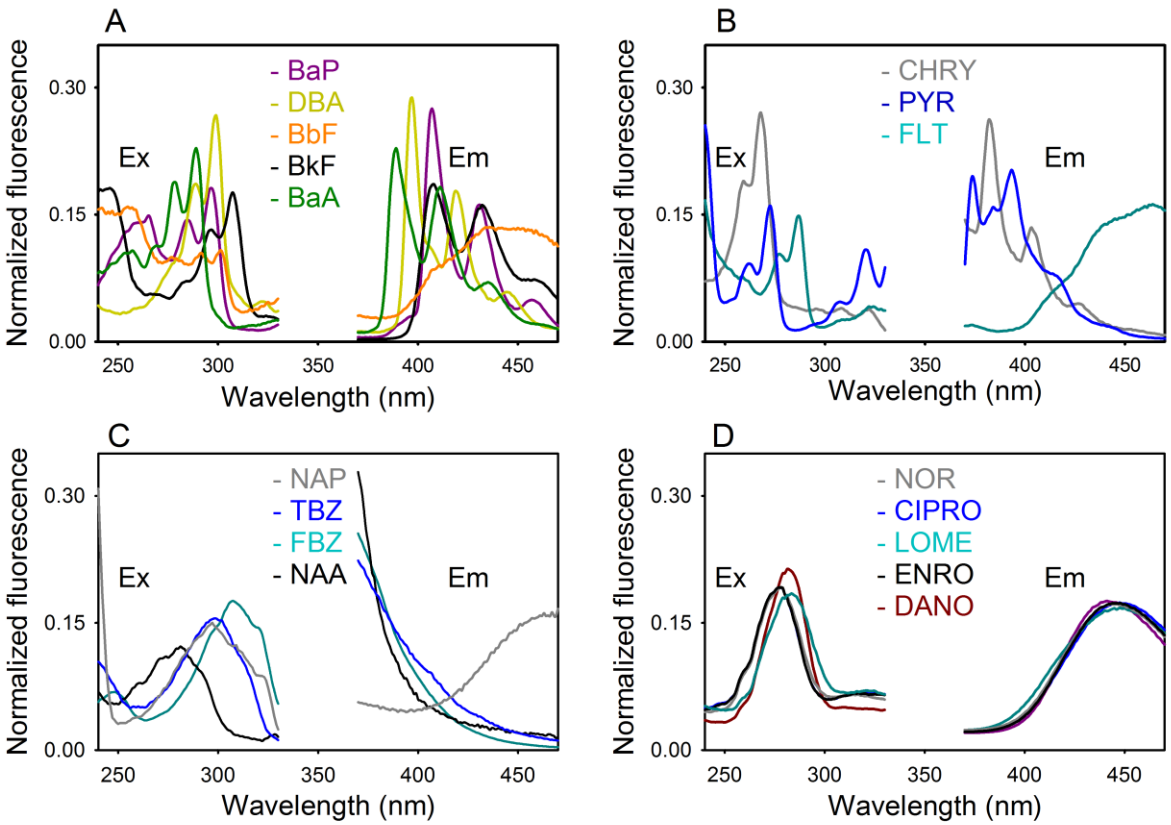
A
- BaP
- DBA
- BbF
- BkF
- BaA
Ex
Em
Normalized fluorescence
0.30
0.15
0.00
250
300
350
400
450
Wavelength (nm)
B
- CHRY
- PYR
- FLT
Ex
Em
Normalized fluorescence
0.30
0.15
0.00
250
300
350
400
450
Wavelength (nm)
C
- NAP
- TBZ
- FBZ
- NAA
Ex
Em
Normalized fluorescence
0.30
0.15
0.00
250
300
350
400
450
Wavelength (nm)
D
- NOR
- CIPRO
- LOME
- ENRO
- DANO
Ex
Em
Normalized fluorescence
0.30
0.15
0.00
250
300
350
400
450
Wavelength (nm)

Figure 4

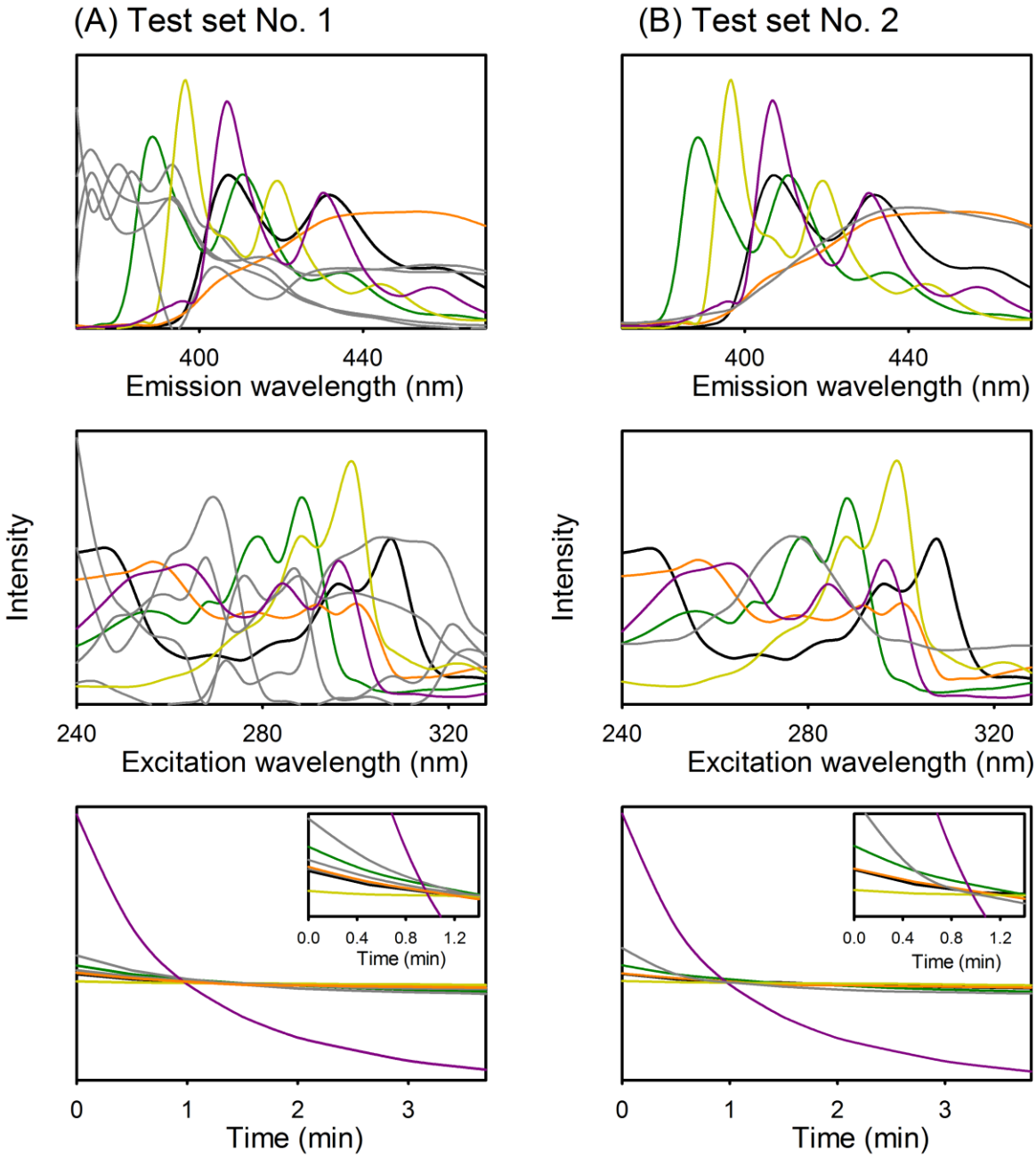
(A) Test set No. 1
(B) Test set No. 2
400
440
Emission wavelength (nm)
Intensity
240
280
320
Excitation wavelength (nm)
0.0
0.4
0.8
1.2
Time (min)
0
1
2
3
Time (min)

Figure 5

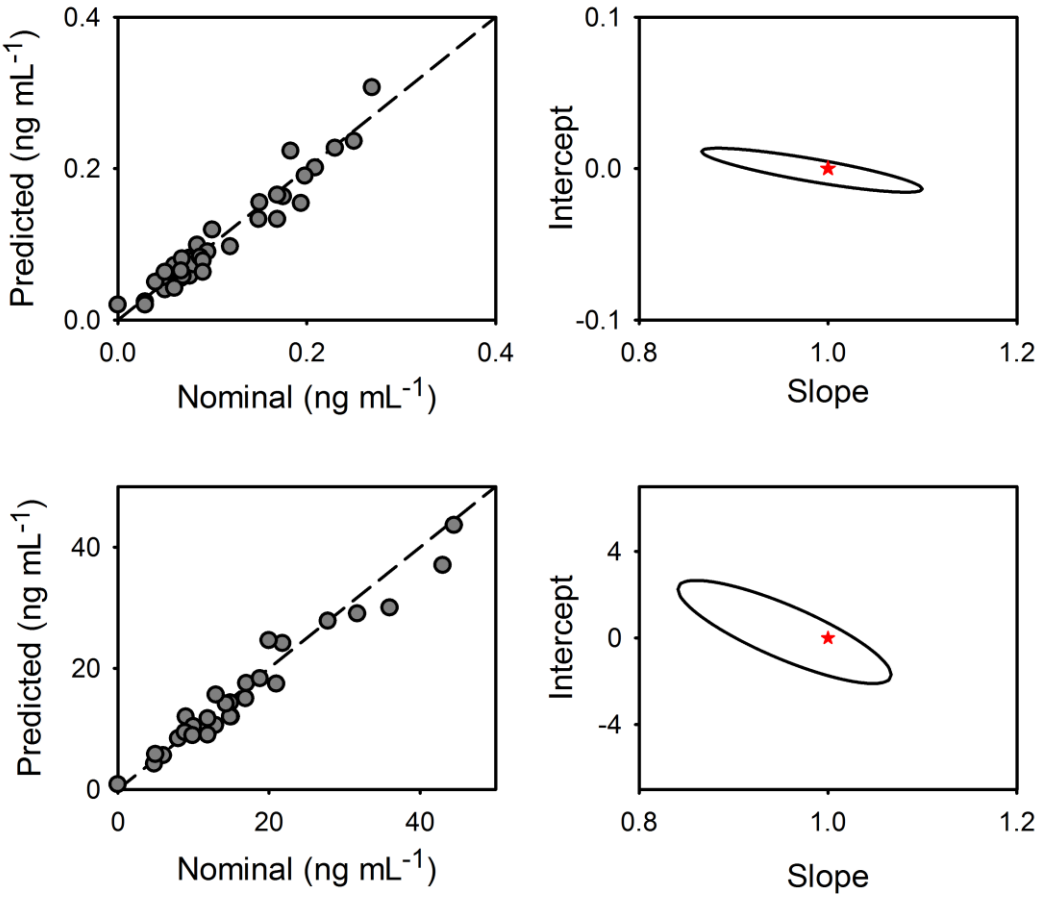
Predicted (ng mL-1)
Nominal (ng mL-1)
Intercept
Slope
0.0
0.2
0.4
-0.1
0.1
0.8
1.0
1.2
0
20
40
-4
4

Figure 6